

Roughness of amorphous Zn-P thin films

BOŻENA JARZĄBEK, JAN JURUSIK, JAN CISOWSKI*

Polish Academy of Sciences, Centre of Polymer Chemistry, P.O. Box 20, 41-819 Zabrze, Poland.

MARIAN NOWAK

Institute of Physics, Silesian University of Technology, P.O. Box 221, 40-019 Katowice, Poland.

The effect of thickness variation and the surface roughness of amorphous $Zn_{32}P_{68}$ thin films has been investigated by the interference spectroscopy of the optical transmittance and reflectance, as well as by the atomic force microscopy (AFM). The analysis of the optical data allowed determination of the standard deviation of the thin film thickness by taking into account the Gaussian distribution of the change in phase of radiation traversing a thin film. It appears that the value of the standard deviation of the film thickness determined from the optical interference spectroscopy ($\sigma_w \approx 26$ nm) is comparable with the value of the mean surface roughness ($R_a \approx 19$ nm) evaluated from the AFM studies.

1. Introduction

The optical parameters, such as the absorption coefficient α and the real part of the refractive index n obtained for thin films, are strongly affected by the film inhomogeneity, resulting in variation of the refractive index Δn , thickness variations Δw , nonparallelism, surface roughness and illumination wavelength bandwidth $\Delta\lambda$. If one takes into account Δn , Δw and $\Delta\lambda$, the second order different equations for electrical and magnetic field strengths in an optical inhomogeneous medium [1] have to be solved. This is, however, difficult and complicated even in a few special cases, when these equations may be solved explicitly. So, since the optical properties of the film are determined by, at least, two parameters, *e.g.*, n and w , it is necessary to take measurements of, at least, the same number of independent properties of the transmitted or/and reflected beams. Multiple angle reflectometry [2], standard ellipsometry [3], optical transmittance $T(\lambda)$ [4]–[6] and reflectance $R(\lambda)$ [7], [8] measurements or simultaneously $T(\lambda)$ and $R(\lambda)$ [9]–[13] data can be used to determine the optical parameters and thickness variations or inhomogeneity of thin films.

As is shown in [4], the influence of film inhomogeneity and surface roughness is significant only in low absorption region, where thickness interferences in $T(\lambda)$ and

*Also, Institute of Physics, Silesian University of Technology, P.O. Box 221, 40-019 Katowice, Poland.

$R(\lambda)$ spectra are observed. The height and position of the transmittance and reflectance minima and maxima change, as compared with the spectra of the ideal, homogeneous, smooth and parallel-sided film, which may lead to too large an absorption coefficient and to erroneous values of refractive index of non-ideal films. Assuming that the envelopes of the spectral interference characteristics of $T(\lambda)$ or $R(\lambda)$ are continuous functions of λ [14], the optical parameters can be evaluated for each wavelength.

The influence of the linear distribution of the change in phase Γ of radiation traversing a thin film on the spectral characteristics $T(\lambda)$ and $R(\lambda)$ has been first considered in [4]. Then, consequences of the linear and Gaussian distributions of Γ for $T(\lambda)$ and $R(\lambda)$ have been discussed [5], [13] showing that the values of geometrical and optical parameters obtained from spectral investigations of $T(\lambda)$ and/or $R(\lambda)$ are more reliable in the second case.

The aim of this paper is to compare results of the interference spectroscopy investigations with the data obtained using the AFM. The latter technique allows one to independently determine the roughness of the free surface. In the case of thin films, it is well known that their properties and structure strongly depend on many deposition conditions, such as the type and roughness of the substrate, rate and angle of deposition, substrate temperature, residual gas pressure, *etc.*; moreover, during the deposition process, the thin film growth structure evolves and projects on the film surface, giving rise to the surface topography [15], [16].

2. Experimental

Thin amorphous films of $\text{Zn}_{32}\text{P}_{68}$, studied in this work, have been obtained by thermal evaporation of the bulk semiconductor ZnP_2 onto the polished and chemically cleaned BK-7 glass substrate. The deposition process was conducted in the vacuum kept at the level of 10^{-3} Pa and the temperature of substrates was about 300 K. The mean film thickness, measured by an interference microscope, was about 0.6 μm and the weight composition of the film was determined by chemical spectroscopy analysis.

The room temperature optical transmittance and reflectance spectra were measured in the range 200–3000 nm, using the Beckman ACTA MIV (UV-VIS-NIR) spectrophotometer [17] and the width of the illumination beam light was about 10×15 mm. The error of transmission and reflection measurements amounted to $\pm 0.5\%$.

The TopoMetrix AFM in contact mode was used in the thin film surface topography investigation. The instrument allows for two methods of obtaining the surface images, namely the variable force method (the internal sensor image) and the constant force method (the topographic image). Both detection methods can be used simultaneously to acquire separately the internal sensor- and topography images.

3. Results and discussion

3.1. Optical determination of geometrical parameters of a thin films

In the present work, we determine the optical transmittance and reflectance of a parallel-sided thin film on a parallel-sided transparent substrate. For the sake of simplicity we make the same assumptions as in [5] and [13]:

1. A thin isotropic semiconductor film covers a thick, non-absorbing substrate immersed in air ($\Delta n \approx 0$).

2. Radiation of wavelength λ , which is perpendicularly incident on the sample, has components in the wavelength range $\Delta\lambda \approx 0$.

3. Interference of internally reflected radiation occurs in a semiconductor film ($\Delta\lambda \ll \lambda^2/(2nw)$) and is negligible in the substrate ($\Delta\lambda \gg \lambda^2/(2n_2w_2)$), where w_2 and n_2 represent the thickness and refractive index of the substrate, respectively.

4. The thickness of the thin film can be different at different points in the illuminated area. The change Δn of the real part of the refractive index of the film (over the illuminated sample area) is negligible, *i.e.*,

$$\frac{\sigma_w}{w} + \frac{\Delta\lambda}{\lambda} \gg \frac{\Delta n}{n} \quad (1)$$

where σ_w is the standard deviation of the film thickness over the illuminated sample area.

5. Taking film thickness and wavelength of radiation as random (see, *e.g.*, [5]), we assume that the change in phase Γ or radiation traversing twice the film is Gaussian.

In consequence, the effective optical transmittance and reflectivity also have the Gaussian distribution and can be calculated using the formulae:

$$T_G = \int_0^{+\infty} \frac{T(\Gamma)}{\sigma_\Gamma \sqrt{2\pi}} \exp\left[-0.5\left(\frac{\Gamma_0 - \Gamma}{\sigma_\Gamma}\right)^2\right] d\Gamma, \quad (2)$$

$$R_G = \int_0^{+\infty} \frac{R(\Gamma)}{\sigma_\Gamma \sqrt{2\pi}} \exp\left[-0.5\left(\frac{\Gamma_0 - \Gamma}{\sigma_\Gamma}\right)^2\right] d\Gamma \quad (3)$$

where $T(\Gamma)$ and $R(\Gamma)$ are the well-known optical transmittance and reflectivity of an ideal parallel-sided thin film on a thick substrate, illuminated with strictly monochromatic radiation (see, *e.g.*, [5], [10]), $\Gamma_0 = 4\pi nw/\lambda$ is the most probable change of phase of the radiation traversing twice the thin film, and w represents the most probable value of the film thickness.

Numerical calculations were done to analyze the influence of σ_w on the spectral characteristics of T and R . Spectral dependences of $n(\lambda)$ and $\alpha(\lambda)$ determined in [5] and [13] were used to perform the calculations. The value of $n_2 = 1.5$ was assumed as the refractive index of the substrate plate. It is obvious that the thin film thickness

influences the position of interference fringes in the spectral characteristics of T and R . However, it does not influence the envelopes of these characteristics for negligible absorption of radiation. Due to an increase of photon energy, *i.e.*, an increase in the absorption coefficient of radiation, the interference fringes vanish in the spectral characteristics of T and R . In consequence, the smooth dependence of T and R on photon energy ($h\nu$) is obtained for greater photon energies. An increase of w shifts the region of smooth $T(h\nu)$ and $R(h\nu)$ characteristics to smaller photon energies.

The shapes of the envelopes of $T(h\nu)$ and $R(h\nu)$ depend strongly on changes of the standard deviation of the film thickness σ_w . An increase of σ_w decreases the amplitude of interference fringes and smooth $T(h\nu)$ and $R(h\nu)$ curves are characteristic of negligible interference of radiation. It is a feature of merit that, for medium values of σ_w , the values of maxima in the spectral characteristics of T and R decrease with increasing $h\nu$, while the values of minima increase, attain a maximum value and then decrease with increasing $h\nu$ (all in the range of negligible absorption of radiation in the sample). This is the main evidence of the influence of the radiation wavelength bandwidth $\Delta\lambda$ and/or changes of thin film thickness and refractive index on the optical transmittance and reflectance.

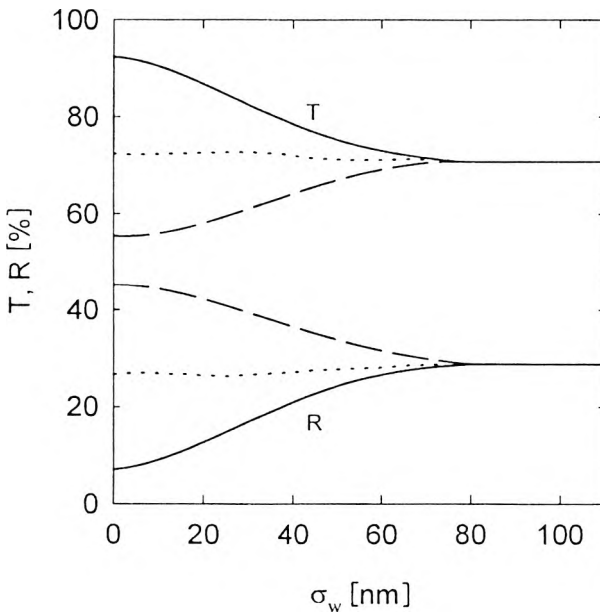


Fig. 1. Influence of thickness variation σ_w on the optical transmittance and reflectance for different thicknesses of a thin film (solid line: $w = 567$ nm, dotted line: $w = 607$ nm, dashed line: $w = 667$ nm, $\alpha = 0$, $\Delta n = 0$, $\Delta\lambda = 0$, $\lambda = 1.03$ μm , $n = 2.74$).

It is very important that, for the Gaussian distribution of Γ , the optical transmission and reflection are monotonic functions of the standard deviation σ_w (Fig. 1). An increase of σ_w does not influence the so-called averaged magnitude

of T and R . This magnitude is strongly dependent on the value of the real part of the refractive index n [5], [13] and, obviously, it depends on the absorption coefficient α . Therefore, the interference spectroscopy of optical transmission and reflection can be used for determination of optical constants, average thickness and standard deviation of its value in illuminated area of thin films.

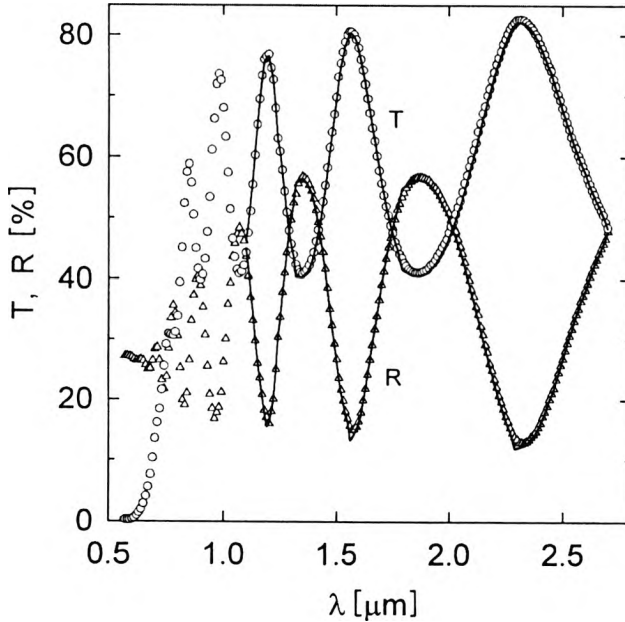


Fig. 2. Spectral dependences of the optical transmittance (circles) and reflectance (triangles) of the 600 nm thick film of $Zn_{32}P_{68}$ evaporated on BK-7 substrate. Solid lines represent the least-squares fitted theoretical dependences for negligible absorption of light; the fitted parameter $\sigma_w = 26$ nm.

To determine the geometrical parameters of the investigated $Zn_{32}P_{68}$ film from $T(\lambda)$ and $R(\lambda)$ data obtained from optical measurements (see Fig. 2), we used the method of experimental data analysis presented in [5], [13]. We were able to apply this method for wavelength above 1000 nm, where the film absorption was weak. For the wavelength below 1000 nm, the influence of band tails absorption seems to be more significant, so that the surface roughness effect is not clearly visible. The optical properties of the film studied have been more extensively discussed in [17]. The effect of bandwidth $\Delta\lambda$ may be negligible in the range we used in our method (*i.e.*, from 1000 to 3000 nm), because in the case of Beckman spectrophotometer $\Delta\lambda \approx 3$ nm, giving in this range, an error from 0.1 to 0.3%, which is in very good agreement with assumption 2.

The value $\sigma_w = 26$ nm was determined by fitting the numerically established envelope of $T(\lambda)$ and $R(\lambda)$ in the range of negligible absorption in the sample. However, in the case of amorphous material, the absorption by levels inside the gap may result in a higher value of σ_w than in reality. The value of thickness $w = 689$ nm

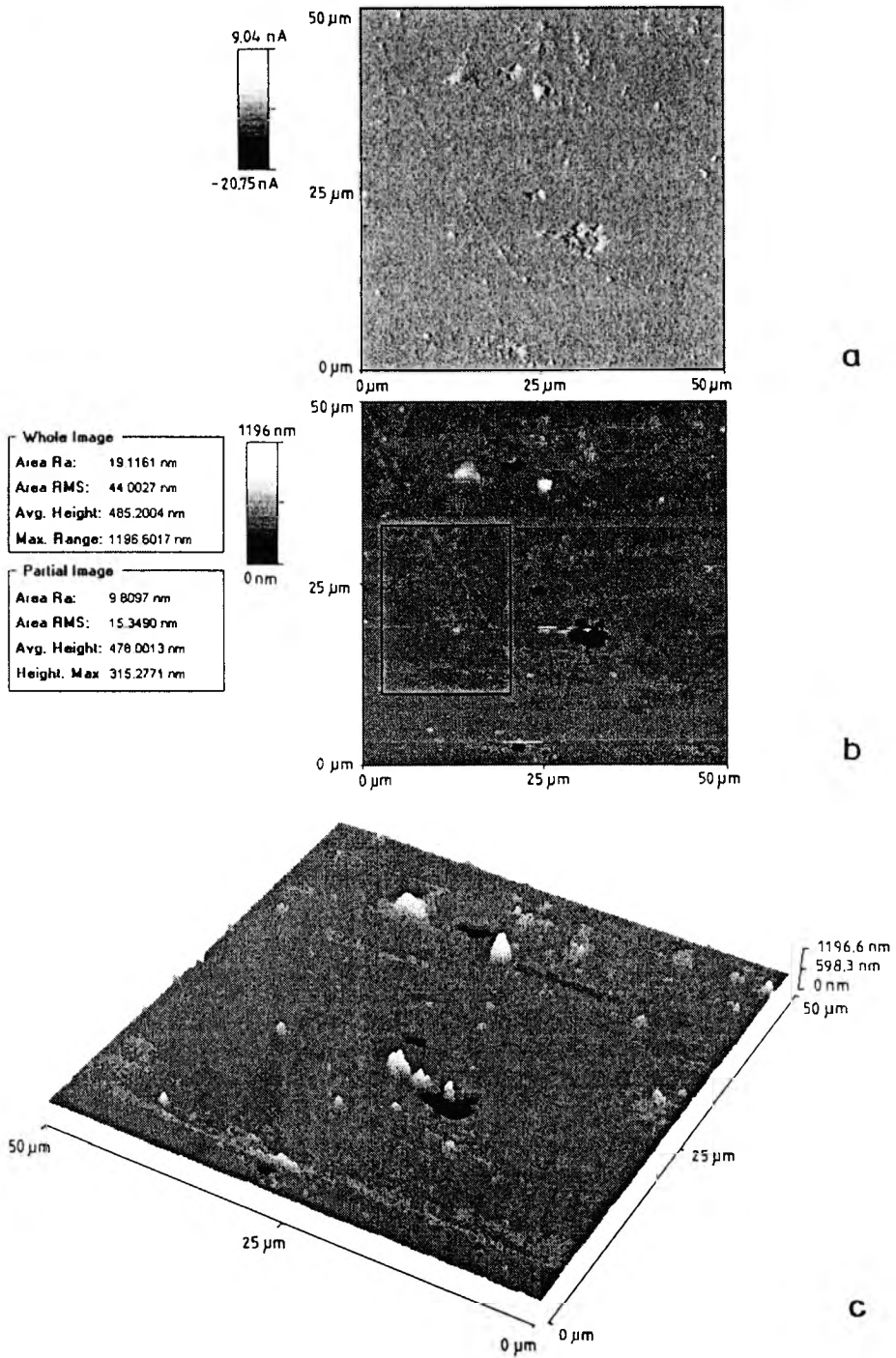


Fig. 3. AFM 50 × 50 nm: **a** – internal sensor, **b** – topography, and **c** – 3D surface images of the 0.6 μm thick $Zn_{32}P_{68}$ amorphous film. Tables contain the area analysis data.

was obtained by fitting the interference fringes of $T(\lambda)$ and $R(\lambda)$ in the same spectral range. Using the known values of σ_w and w , the values of $n(h\nu)$ and $\alpha(h\nu)$ were found numerically by fitting the spectral characteristics of optical transmittance and reflectance and their envelopes in the range of small absorption of radiation. The theoretical transmission and reflectance calculated for thus determined σ_w , w , $n(h\nu)$ and $\alpha(h\nu)$ are shown as solid lines in Fig. 2, describing satisfactorily the experimental data.

3.2. Atomic force microscopy studies

Figure 3 shows subsequently: sensor (a), topography (b), and three-dimensional (3D) (c) topography $50 \times 50 \mu\text{m}$ images of the amorphous $\text{Zn}_{32}\text{P}_{68}$ film surface. The surface of the film is flat with roughness (protrusions, irregular holes, scratches and streaks) arising mainly from both the growth structure (which can also be related to the substrate surface inhomogeneity) as demonstrated in [18] and post-deposition treatment (*e.g.*, scratches). The shadows that clearly appear on the 3D topography image as a real structure can be attributed to the interaction of the AFM probe tip with a large surface irregularity (spikes and holes) [19]. In addition, tables in Fig. 3 contain the area standard roughness data calculated with the AFM device for whole and partial micrograph areas. The mean surface roughness R_a over the whole image area was about 19 nm, being equal to about 9 nm in the partial image area without the large surface inhomogeneity. When viewed on the larger surface area, the film exhibits considerably more roughness.

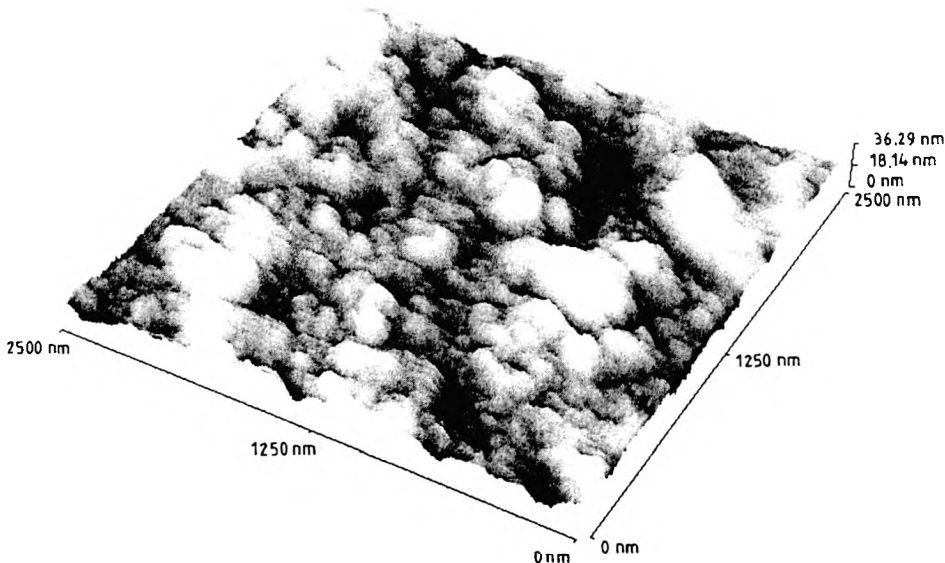


Fig. 4. AFM $2500 \times 2500 \text{ nm}$ 3D-topography image of the amorphous $\text{Zn}_{32}\text{P}_{68}$ thin film surface.

Figure 4 presents the $2500 \times 2500 \text{ nm}$ film surface area of the same film. The surface almost entirely consists of dome-like shaped agglomerates. Such a surface structure (topography) in amorphous films may be associated with the internal growth structure

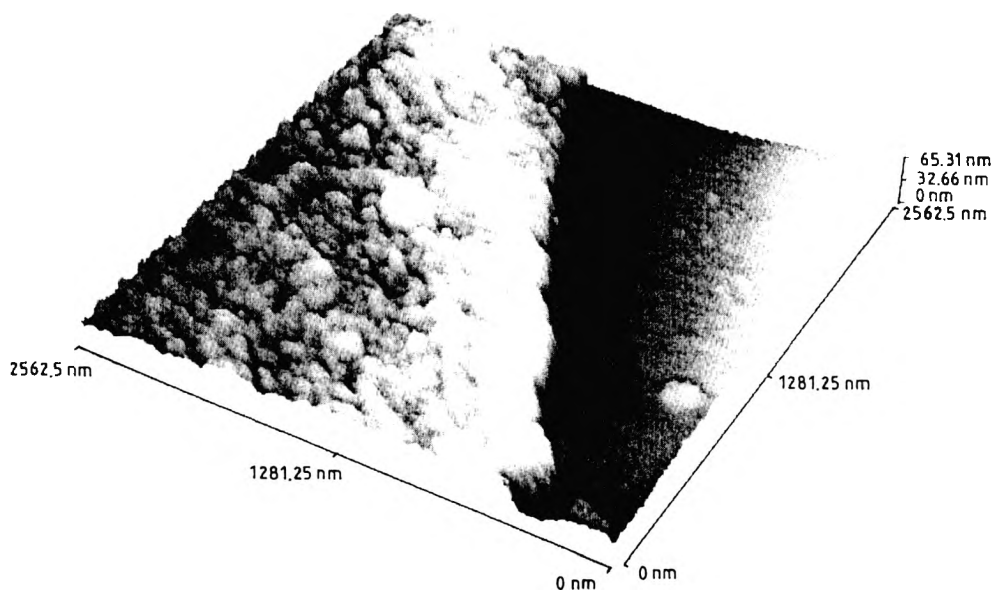


Fig. 5. AFM 3D-topography image of the amorphous $\text{Zn}_{32}\text{P}_{68}$ film edge (the cross-section) growing closely to the mask edge during the deposition process.

as follows from Fig. 5, where the edge of the film (the cross-section), growing closely to the mask edge during the deposition process, is shown. An interesting feature of the film studied is that, being amorphous, it exhibits a pronounced structure in the form of density fluctuations, known also as the “columnar growth structure”, the term typically used for crystalline films [15]. Often, some perturbations of the growth structure (called the growth defects [20]), such as those shown in Fig. 3c (large spikes) appear and contribute to a higher film surface roughness.

4. Conclusions

Applying numerical least-square fitting of $T(h\nu)$ and $R(h\nu)$ to the theoretical dependences which take into account the Gaussian distribution of the change in phase Γ of radiation traversing a thin film, the geometrical parameters of such a film can be determined. This method allows determination of the thickness of a thin film and its standard deviation over the illuminated sample area. The geometrical parameters of $\text{Zn}_{32}\text{P}_{68}$ thin film evaluated from the interference spectroscopy of $T(h\nu)$ and/or $R(h\nu)$ are comparable with those obtained from the AFM studies. In particular, the value of the standard deviation of the film thickness determined from the optical interference spectroscopy ($\sigma_w \approx 26$ nm) is quite reasonable, taking account the value of the mean surface roughness ($R_a \approx 19$ nm) evaluated from the AFM studies.

Acknowledgments — This work was partially supported by the Silesian University of Technology, Gliwice, Poland, under contract BK-65/RMF-1/99.

References

- [1] KNITTL Z., *Optics of Thin Films*, Wiley, London 1976.
- [2] TAYLOR D.F., Jr., NELSON W.T., LIVINGSTON R.S., *Multiple Angle Reflectometric Thickness Measurement Techniques*, AIXC Application Rep.
- [3] AZZAM R.M., BASHARA N.M., *Ellipsometry and Polarized Light*, North-Holland, Amsterdam 1992.
- [4] SWANEPOEL R., *J. Phys. E* **17** (1984), 896.
- [5] NOWAK M., *Thin Solid Films* **254** (1995), 200.
- [6] BAH K., CZAPLA A., PISARKIEWICZ T., *Thin Solid Films* **232** (1993), 18.
- [7] HEAVENS O.S., *Optical Properties of Thin Solid Films*, Dover Publ., New York 1965.
- [8] JEZIEWSKI K., MISIEWICZ J., *Opt. Commun.* **65** (1988), 217.
- [9] JARZĄBEK B., WESZKA J., JURUSIK J., CISOWSKI J., *Electron Technology* **20** (1997), 193.
- [10] PISARKIEWICZ T., STAPINSKI T., CZTERNASTEK H., RAVA P., *J. Non-Cryst. Solids* **137/138** (1991), 619.
- [11] SZCZYRBOWSKI J., *J. Phys. D: Appl. Phys.* **11** (1978), 583.
- [12] SZCZYRBOWSKI J., CZAPLA A., *J. Phys. D: Appl. Phys.* **12** (1979), 1737.
- [13] KĘPIŃSKA M., NOWAK M., *NDT&E International (Independent Nondestructive Testing and Evaluation)* **31** (1998), 105.
- [14] MANIFACIER J.C., GASLOT J., FILLARD J.P., *J. Phys. E: Sci. Instrum.* **17** (1984), 896.
- [15] JURUSIK J., *Thin Solid Films* **214** (1992), 117.
- [16] THORNTON J.A., *Ann. Rev. Mater. Sci.* **7** (1977), 239.
- [17] JARZĄBEK B., WESZKA J., BURIAN A., POCZTOWSKI G., *Thin Solid Films* **297** (1996), 204.
- [18] RUPPE C., DUPARRE A., *Thin Solid Films* **288** (1996), 8.
- [19] LENIHAM T.G., MALSHE A.P., BROWN W.D., SCHAPER L.W., *Thin Solid Films* **270** (1995), 356.
- [20] SPALVINS T., *Thin Solid Films* **64** (1979), 143.

*Received December 6, 1999
in revised form April 27, 2000*